

Self-Consistent Single-Particle Simulation

F. M. Bufler, C. Zechner,* A. Schenk, and W. Fichtner

Institut für Integrierte Systeme, ETH Zürich

Gloriastrasse 35, CH-8092 Zürich, Switzerland

E-mail: bufler@iis.ee.ethz.ch

* ISE Integrated Systems Engineering AG

Balgriststrasse 102, CH-8008 Zürich, Switzerland

Abstract— Self-consistent single-particle Monte Carlo device simulations are presented. Self-consistency is achieved by an iterative coupling-scheme of single-particle frozen-field Monte Carlo simulations with solutions of the nonlinear Poisson equation. As an example a realistic $0.1 \mu\text{m}$ n-MOSFET obtained from process simulation with maximum doping levels of about $2.5 \times 10^{20} \text{ cm}^{-3}$ is simulated. It is found that the resulting drain current is independent of the length of the time interval per iteration (provided that it is not too small) and independent of the density in the regions not visited by the particles taken either from a drift-diffusion or a hydrodynamic simulation. Therefore self-consistent single-particle Monte Carlo simulation is an accurate and robust simulation tool for the quasi-ballistic regime in sub $0.1 \mu\text{m}$ MOSFETs.

I. INTRODUCTION

As silicon MOSFETs are scaled into the sub $0.1 \mu\text{m}$ regime, the on-current I_{on} is increasingly influenced by quasi-ballistic transport which is not adequately taken into account by standard drift-diffusion (DD) or hydrodynamic (HD) device simulation [1], [2]. An approach capable of incorporating accurately ballistic effects is self-consistent full-band Monte Carlo (FBMC) simulation [3]. However, the stability of the standard self-consistency scheme for ensemble FBMC simulations requires very small time steps for the Poisson updates [4]. Higher doping levels necessitate smaller time steps [4] and hence decrease the CPU time efficiency. Therefore, most of the recent ensemble FBMC simulations were restricted to device structures with a maximum doping level considerably or even far below $1 \times 10^{20} \text{ cm}^{-3}$ [5], [6], [7], whereas the doping concentration is above this level in the source/drain regions of realistic MOSFETs. The stability problem does not oc-

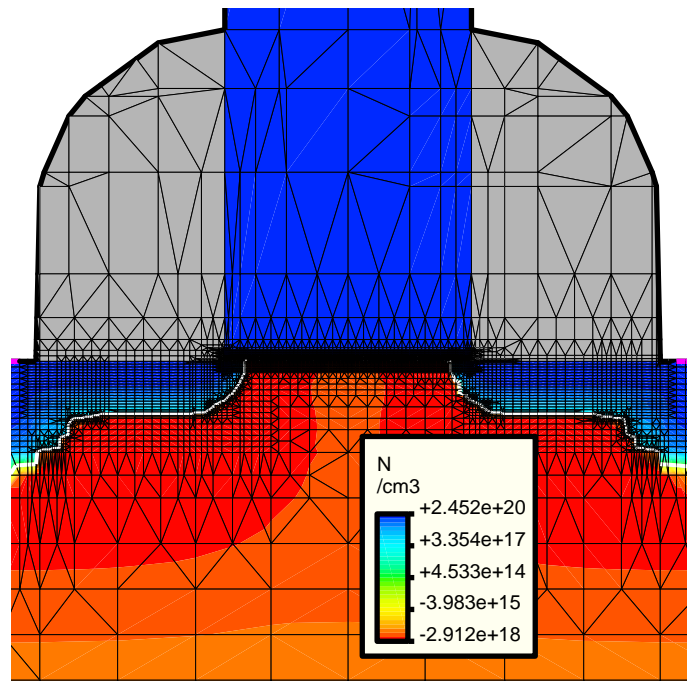


Fig. 1. Simulated n-MOSFET with $L_{\text{ch}} = 90 \text{ nm}$, $L_{\text{eff}} = 75 \text{ nm}$ and $t_{\text{ox}} = 2.2 \text{ nm}$. The white lines indicate the pn junctions.

cur for an iteration scheme, where frozen-field MC simulations are coupled with solutions of the nonlinear Poisson equation [8]. It is the aim of this paper to combine these self-consistency iterations [8] with efficient single-particle FBMC simulations [9], to examine the validity of this approach and to demonstrate its feasibility as well as its efficiency for the simulation of a realistic $0.1 \mu\text{m}$ nMOSFET.

II. SIMULATION APPROACH AND DEVICE STRUCTURE

The details of the single-particle approach (SPARTA) to FBMC device simulation regarding the propagation algorithm as well as the models

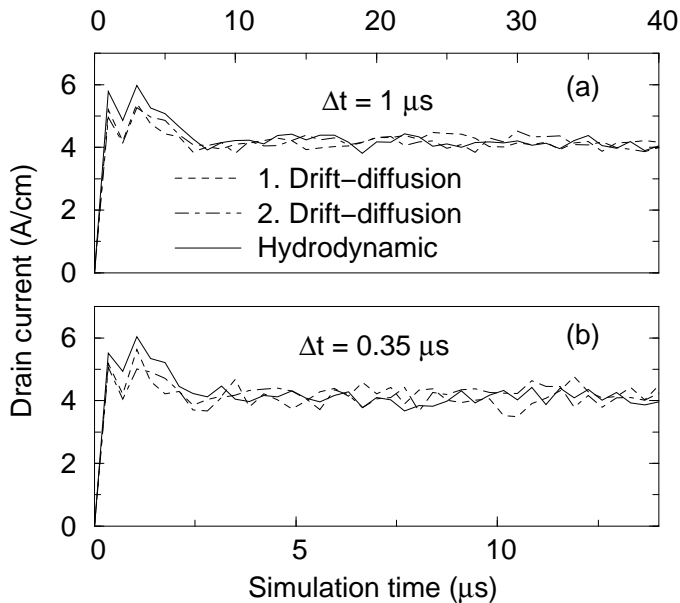


Fig. 2. Drain current as a function of simulation time when using a time step per frozen-field iteration of (a) $\Delta t = 1 \mu s$ and (b) $\Delta t = 0.35 \mu s$. Three simulation runs are shown based on an initial drift-diffusion or a hydrodynamic simulation.

for band structure and scattering mechanisms are reported in Ref. [9]. Recent modifications include a finer discretization of \mathbf{k} -space with a spacing of $1/96 \times 2 \pi/a$ ($a =$ lattice constant) and the injection of the electron from a contact which is now chosen from a velocity-weighted Maxwellian. The $0.1 \mu m$ nMOSFET was obtained by process simulation and is shown in Fig. 1. It features a channel length of $L_{ch} = 90$ nm, an effective gate length of $L_{eff} = 75$ nm, a physical oxide thickness of $t_{ox} = 2.2$ nm, and a maximum doping level of about $2.5 \times 10^{20} \text{ cm}^{-3}$.

The simulation procedure is as follows. A single-particle is injected from some contact and is propagated in a frozen electric field (initially taken from the DD or HD device simulation), until it is absorbed at a contact. Then the next particle is simulated and so on. If the cumulative simulation time (for all consecutively simulated particles) reaches the end of a predefined time interval Δt , the nonlinear Poisson equation is solved. The density determining the quasi-Fermi potential in the nonlinear Poisson equation [8] is taken from the Monte Carlo density if the real-space element was visited by MC particles or otherwise equals the density of the DD or HD device simulation. After the Poisson equation is solved, the single-particles

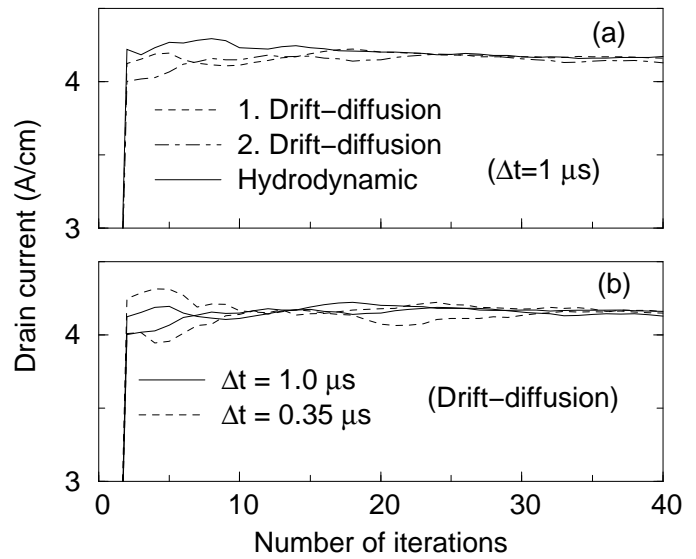


Fig. 3. Cumulative averages of the drain current as a function of iterations after reaching steady state. The dependence on (a) simulation runs and kind of initial simulation (DD or HD) and (b) time interval lengths per iteration is illustrated.

are simulated in the new electric field until the end of the second time interval and the whole procedure is repeated during the Monte Carlo device simulation.

III. VERIFICATION

After the end of each time interval, the drain current I_D is estimated based on the density and the drift velocity obtained in this time interval. The drain current according to three simulation runs at the bias point $V_{DS}=V_{GS}=1.2$ V (two based on an initial DD and one on a HD simulation) is shown in Fig. 2 as a function of the simulation time for two different lengths of the time interval Δt . It can be seen that after ten iterations, i.e. a simulation time of $10 \times \Delta t$, I_D begins to fluctuate around its stationary value. The fluctuations are, of course, stronger for the smaller Δt , but the simulation time for reaching the steady state is shorter. In addition, one can observe that the initial "overshoot" is higher when starting from a HD simulation. After reaching the steady-state, i.e. after ten iterations, cumulative averages can be taken over the I_D values computed after each time interval. The cumulative averages taken over the results shown in Fig. 2 are displayed in Fig. 3 as a function of the iterations following steady-state. In Fig. 3 (a), one observes that the differ-

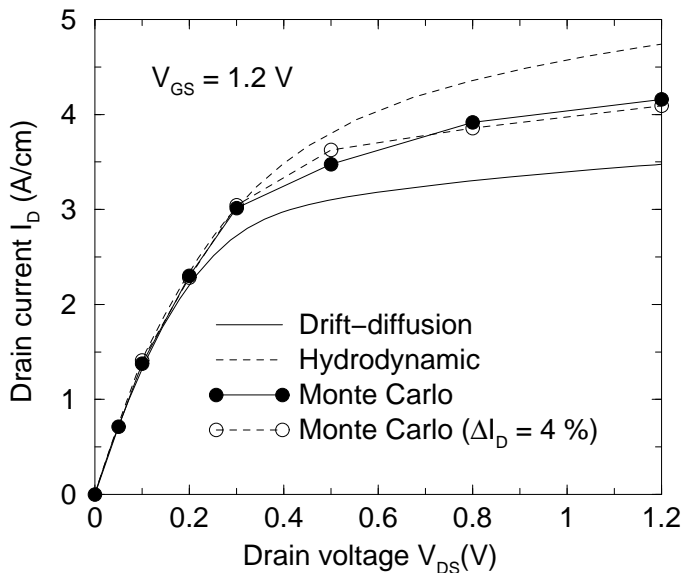


Fig. 4. Output characteristics of the n-MOSFET as computed by the drift-diffusion, hydrodynamic and Monte Carlo model. Monte Carlo simulations terminated by a stopping criterion are also compared to long simulations with negligible error.

ent simulation runs converge to the same solution, regardless of whether DD or HD was taken as initial simulation. It can be concluded that the density in the bulk region, which is never visited by a single-particle and which differs between HD and DD, has a negligible effect on the Poisson equation. Figure 3 (b) shows that the same solution is also obtained for different Δt . Consequently, the smaller Δt is to be preferred since steady-state is reached earlier (but, of course, Δt must not be too small so that even regions inside the inversion channel are not visited).

IV. SIMULATION RESULTS

In Fig. 4, the output characteristics of the MOSFET are shown as resulting from the DD, HD and FBMC model, respectively. In addition, FBMC simulations starting from DD with $\Delta t = 0.35 \mu s$ and averaging after 5 iterations are included where the simulations are stopped below a "relative error" of 4 % for I_D . The corresponding six points on the I_D - V_D curve took 31,5 h CPU time on two 667 MHz alpha processors. Of course, the I_D values are not strictly independent as for frozen-field MC simulations [10], but from a practical point of view ΔI_D is nevertheless a useful stopping criterion for discriminating between the different CPU

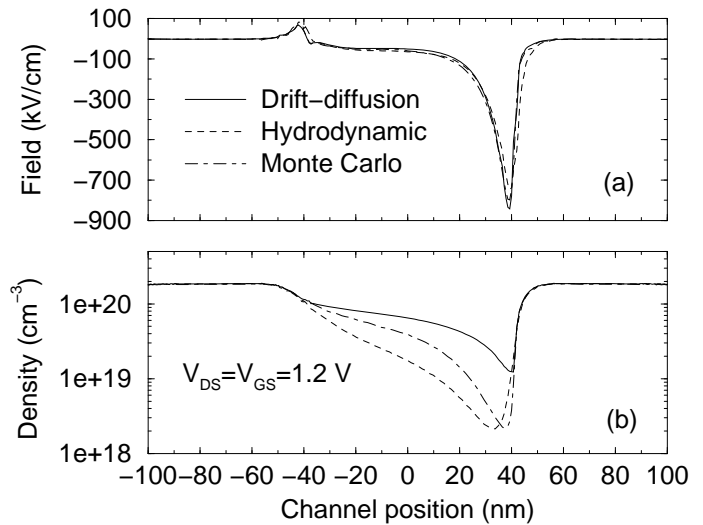


Fig. 5. (a) Longitudinal electric field and (b) electron density profiles along the channel. Both quantities are averaged perpendicularly to the Si/SiO₂ interface by the electron density.

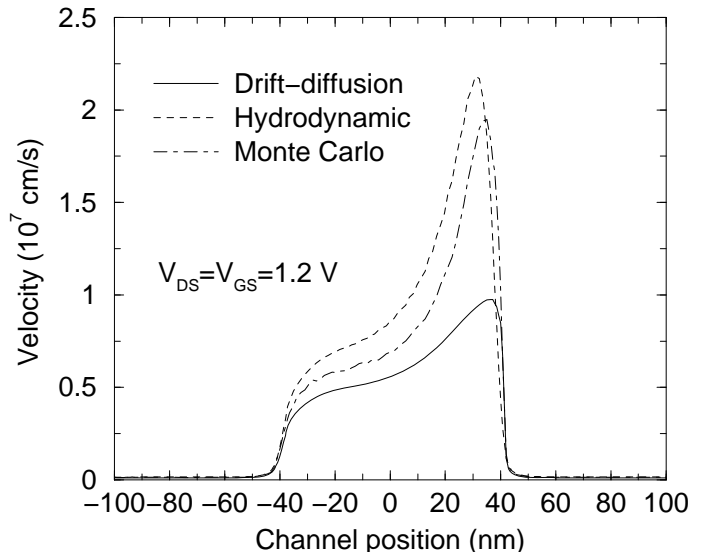


Fig. 6. Electron drift velocity, averaged perpendicularly to the Si/SiO₂ interface by the electron density, as a function of channel position.

times necessary for similar accuracy at different bias points. Finally, as an illustration of the simulation results, the channel profiles for longitudinal field, electron density and drift velocity are shown in Figs. 5 and 6 with the different source-side velocities as origin for the different I_{on} .

V. CONCLUSIONS

In conclusion, self-consistent FBMC results were obtained by an iterative coupling of single-

particle simulations with a nonlinear Poisson solver. The validity and efficiency was demonstrated by simulations of a realistic $0.1\ \mu\text{m}$ nMOS-FET thus making FBMC a viable part of TCAD for nanoscale MOSFETs.

ACKNOWLEDGMENT

This work was in part supported by the Kommission für Technologie und Innovation under Contract 4082.2.

REFERENCES

- [1] K. Banoo and M. S. Lundstrom, "Electron transport in a model Si transistor," *Solid-State Electron.*, vol. 44, pp. 1689–1695, 2000.
- [2] J. D. Bude, "MOSFET modeling into the ballistic regime," in *Proc. SISPAD*, Seattle (U.S.A.), Sept. 2000, pp. 23–26.
- [3] M. V. Fischetti and S. E. Laux, "Monte Carlo analysis of electron transport in small semiconductor devices including band-structure and space-charge effects," *Phys. Rev. B*, vol. 38, pp. 9721–9745, 1988.
- [4] P. W. Rambo and J. Denavit, "Time stability of Monte Carlo device simulation," *IEEE Trans. Computer-Aided Des.*, vol. 12, pp. 1734–1741, 1993.
- [5] A. Duncan, U. Ravaioli, and J. Jakumeit, "Full-band Monte Carlo investigation of hot carrier trends in the scaling of metal-oxide-semiconductor field-effect transistors," *IEEE Trans. Electron Devices*, vol. 45, pp. 867–876, 1998.
- [6] C. Jungemann, S. Keith, M. Bartels, and B. Meinerzhagen, "Efficient full-band Monte Carlo simulation of silicon devices," *IEICE Trans. Electron.*, vol. E82–C, pp. 870–879, 1999.
- [7] W. J. Gross, D. Vasileska, and D. K. Ferry, "Ultrasmall MOSFETs: The importance of the full Coulomb interaction on device characteristics," *IEEE Trans. Electron Devices*, vol. 47, pp. 1831–1837, 2000.
- [8] F. Venturi, R. K. Smith, E. C. Sangiorgi, M. R. Pinto, and B. Riccò, "A general purpose device simulator coupling Poisson and Monte Carlo transport with applications to deep submicron MOSFET's," *IEEE Trans. Computer-Aided Des.*, vol. 8, pp. 360–369, 1989.
- [9] F. M. Bufler, A. Schenk, and W. Fichtner, "Efficient Monte Carlo device modeling," *IEEE Trans. Electron Devices*, vol. 47, pp. 1891–1897, 2000.
- [10] F. M. Bufler, A. Schenk, and W. Fichtner, "Efficient Monte Carlo device simulation with automatic error control," in *Proc. SISPAD*, Seattle (U.S.A.), Sept. 2000, pp. 27–30.